

Floquet topological $d + id$ superconductivity induced by chiral many-body interactions

Sota Kitamura¹ and Hideo Aoki^{2,3}

¹*Department of Applied Physics, The University of Tokyo, Hongo, Tokyo, 113-8656, Japan*

²*Department of Physics, University of Tokyo, Hongo, Tokyo 113-0033, Japan*

³*Electronics and Photonics Research Institute, Advanced Industrial Science and Technology (AIST), Tsukuba, Ibaraki 305-8568, Japan*

(Dated: July 9, 2022)

We study how d -wave superconductivity is changed when illuminated by circularly-polarised light (CPL) in the repulsive Hubbard model in the strong-coupling regime. We adopt the Floquet formalism for the Gutzwiller-projected effective Hamiltonian with the time-periodic Schrieffer-Wolff transformation. We find that CPL induces a topological superconductivity with a $d + id$ pairing, which arises from the chiral spin coupling and the three-site term generated by the CPL. The latter effect remains significant even for low frequencies and low intensities of the CPL. This is clearly seen in the obtained phase diagram against the laser intensity and temperature for various frequencies red-detuned from the Hubbard U , with the transient dynamics also examined. The phenomenon revealed here can provide a novel way to induce a topological superconductivity.

I. INTRODUCTION

It has become one of the key pursuits in the condensed-matter physics to design new quantum phases as exemplified by unconventional superconductivity and topological states. Conventionally, materials design is the accepted way, in which we tailor the crystal structures, constituent elements, as combined, if necessary, with carrier doping, pressure applications, etc. An entirely different avenue should be a “non-equilibrium design”, in which we envisage to realise interesting quantum phases by putting the systems out of equilibrium, typically by illuminating intense laser lights. This opens an in-situ way to convert the system that would be unthinkable in equilibrium, and is also of fundamental interests as non-equilibrium physics. Ilya Prigogine, in his book *From being to becoming*¹, once said that he would have liked to entitle the book as *Time, the forgotten dimension*, and we can indeed enlarge our horizon if we do not forget the temporal dimension.

One of the most important pathways is the Floquet physics, with which we can seek various novel quantum states arising from application of AC modulations to the system. This is based on Floquet’s theorem put forward by Gaston Floquet in 1883 for time-periodic modulations, which is much older than 1928 theorem by Bloch for spatially-periodic modulations. A prime application of Floquet physics is the “Floquet topological insulator” proposed by Takashi Oka and one of the present authors in 2009²⁻⁴. Namely, by applying a circularly-polarised light to honeycomb systems such as graphene [see Fig. 1a], we can turn the system into a topological insulator in a dynamical manner. In other words, we are here talking about matter-light combined states, since the electron is converted into a superposition of the original, one-photon dressed, two-photon dressed, ..., electrons in the Floquet picture. The Floquet topological insulator with a topological gap exhibits a DC Hall effect despite the modulation being AC. The resulting state is a kind of quantum anomalous Hall effect (i.e., quantum Hall effect in zero magnetic field) originally proposed for the static case by Duncan Haldane back in 1988⁵. Indeed, the effective Hamiltonian for the irradiated system in the leading order in the Floquet formalism exactly coincides with Haldane’s model [Fig. 1b], as shown by Takuya Kitagawa et al.⁶

2019 witnessed an experimental detection of the Floquet topological insulator in graphene by James McIver et al.⁷

Thus there arose a surge of interests in Floquet topological phases, for many-body problems as well as one-body cases. Floquet physics has also been extended to explore superconductivity in AC-modulated situations. It is out of the scope of the present paper to review them, but the many-body interests include

topology	superconductivity
FTI \leftrightarrow Mott’s insulator	Attraction-repulsion conversion
chiral spin states	η -pairing

to just name a few. Namely, by considering the illuminated repulsive Hubbard model for correlated electrons we can show a phase diagram, where transitions appear between the Floquet topological insulator (FTI) and Mott’s insulator.⁸ In the strong-coupling case, where the repulsion U is much greater than the electron hopping t_0 , strange magnetic states such as chiral spin states can be induced by circularly-polarised laser lights [see Fig. 1c,1d]⁹⁻¹² due to the emergence of a scalar spin-chiral coupling ($\hat{S}_i \times \hat{S}_j \cdot \hat{S}_k$). There, we realised that Floquet-incuded chiral coupling becomes significant when the frequency ω of the laser is *on-resonant with the Hubbard U* , with vastly different behaviours between the cases when ω is slightly red-detuned from U and blue-detuned.

For superconductivity on the other hand, we can convert between repulsive and attractive interactions by applying (linearly-polarised) laser.¹³ η -pairing (condensation of pairs at Brillouin zone corners) is also proposed to arise from (linearly-polarised) laser.¹⁴ There, the Floquet effective pair-hopping becomes significant when ω is again on-resonant with U , with different behaviours between ω red-detuned or blue-detuned from U .

Now the purpose of the present paper is to encompass topological and superconducting properties to seek whether a “Floquet-induced topological superconductivity” can arise. While there have been various attempts at realising Floquet topological superconducting states¹⁵⁻¹⁹, an obstacle is the fact that the pairing symmetry is hard to be controlled in a direct manner, since the gap function does not couple to electromagnetic fields. Thus, usually, we have to prepare some specific

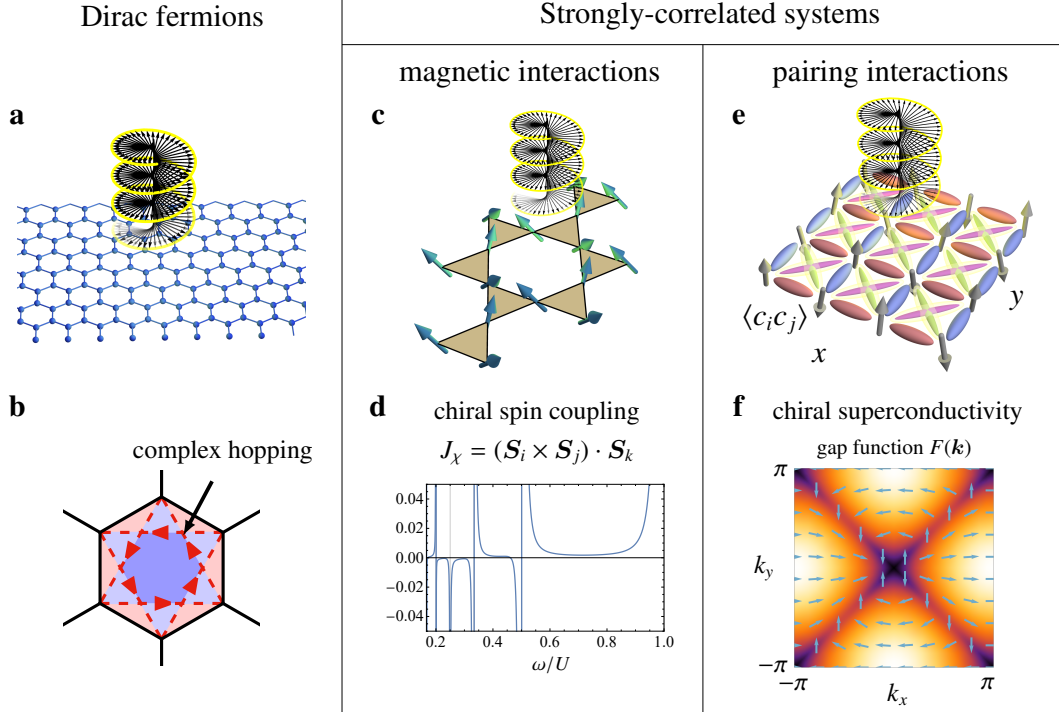


Fig. 1. **Various Floquet-induced quantum states.** For Dirac fermions as in graphene, **a** illumination of a circularly-polarised light (CPL) induces the Floquet topological insulator, which arises from photon-assisted complex hopping (**b**), where colour shadings represent the piecewise magnetic fluxes. **c** For magnetic phases in strongly-correlated systems, illumination of CPL gives rise to a chiral spin coupling, for which **d** illustrates a resonant behaviour at $\omega/U = 1, 1/2, 1/3, \dots$. For superconductors, **e** illumination of CPL on a $d_{x^2-y^2}$ -wave superconductor produces pairing amplitudes $\langle \hat{c}_i \hat{c}_j \rangle$ across nearest neighbours (red: positive; blue: negative) along with imaginary diagonal bonds (magenta and green), leading to an emergent complexified gap function $F(\mathbf{k})$, and we have a photo-induced chiral $d + id$ superconductivity (**f**), where arrows schematically indicate the phase of the gap function.

band structures in order to induce a topological transition or to change the pairing symmetry drastically. Instead, the strategy of the present paper is to illuminate a circularly-polarised light (CPL) to the repulsive Hubbard model in the strong-coupling regime to exploit the peculiar CPL-induced interactions emergent in that regime. We shall indeed show that a $d_{x^2-y^2}$ -wave superconductor is changed into a topological $d_{x^2-y^2} + id_{xy}$ wave one [Fig. 1f]. This will be shown in the Floquet formalism for the Gutzwiller-projected effective Hamiltonian with the time-periodic Schrieffer-Wolff transformation. The $d + id$ pairing is in fact shown to arise from the chiral spin coupling and the three-site term caused by the CPL [Fig. 1e]. The latter effect turns out to remain significant even for low frequencies and low intensities of the CPL. This will be summarised in a phase diagram against the laser intensity and temperature for various frequencies red-detuned from the Hubbard U , along with transient dynamics.

II. RESULTS

A. Low-energy effective Hamiltonian

We take in the present study the hole-doped Mott insulator on a square lattice, which is irradiated by an intense circularly-

polarised light (CPL). This can be minimally modelled by the repulsive Hubbard model, with a Hamiltonian

$$\hat{H}(t) = - \sum_{ij\sigma} t_{ij} e^{-i\mathbf{A}(t) \cdot \mathbf{R}_{ij}} \hat{c}_{i\sigma}^\dagger \hat{c}_{j\sigma} + \frac{U}{2} \sum_i \hat{n}_i (\hat{n}_i - 1), \quad (1)$$

where $\hat{c}_{j\sigma}$ annihilates an electron on the site at \mathbf{R}_j with spin $\sigma = \uparrow, \downarrow$, and $\hat{n}_i = \sum_\sigma \hat{n}_{i\sigma} = \sum_\sigma \hat{c}_{i\sigma}^\dagger \hat{c}_{i\sigma}$ is the density operator. For a square lattice the site index j takes the form of $j = mx + ny$ for $\mathbf{R}_j = (ma, na)$ with a being the lattice constant. For the hopping amplitude t_{ij} , here we consider the second-neighbour (t'_0) as well as the nearest-neighbour hopping (t_0), as necessitated for realising a CPL-induced topological superconductivity [as we shall see below Eq. (16)]. The onsite repulsion is denoted as $U (> 0)$.

The circularly-polarised laser field is introduced via the Peierls phase, which involves $\mathbf{R}_{ij} \equiv \mathbf{R}_i - \mathbf{R}_j$, and the vector potential,

$$\mathbf{A}(t) = \frac{\mathbf{E}}{2i\omega} e^{-i\omega t} - \frac{\mathbf{E}^*}{2i\omega} e^{i\omega t}, \quad (2)$$

$$\mathbf{E} = E(1, i) \quad (3)$$

for the right-circularly polarised case; replace \mathbf{E} with \mathbf{E}^* for the left circulation. We set $\hbar = e = 1$ hereafter.

Since the electric field introduced above is time-periodic, $\hat{H}(t + 2\pi/\omega) = \hat{H}(t)$, we can employ the Floquet formalism²⁰, where the eigenvalue, called quasienergy, of the discrete time translation plays a role of energy. Because the quasienergy spectrum is invariant under the time-periodic unitary transformation, $e^{-i\hat{\Lambda}(t)}$ with $\hat{\Lambda}(t + 2\pi/\omega) = \hat{\Lambda}(t)$, we can introduce an effective static Hamiltonian \hat{H}_F as

$$\hat{H}_F = e^{i\hat{\Lambda}(t)}(\hat{H}(t) - i\partial_t)e^{-i\hat{\Lambda}(t)}, \quad (4)$$

where $\hat{\Lambda}(t)$ is determined such that \hat{H}_F becomes time-independent.

Here, a bit of general remark is in order: For continuously-driven closed many-body systems in the thermodynamic limit, the genuine steady state must be at an infinite temperature, which is reflected to the Floquet effective Hamiltonian \hat{H}_F in that the exact eigenstates of \hat{H}_F are featureless^{21,22}. However, this does not rule out the possibility to have a nontrivial long-lived state during the time evolution towards the infinite temperature. In particular, in various situations \hat{H}_F can have an asymptotic expansion with a nontrivial structure, with which the time evolution of the system may be accurately reproduced for a long time. For instance, when the driving frequency ω is high enough, one can obtain \hat{H}_F in an $1/\omega$ expansion^{8,23,24}. The truncated asymptotic series describes the nontrivial long-lived state as a ground state, while the slow heating towards the infinite temperature is separately described by the difference between the truncated series and the true solution^{25,26}.

The slow heating is expected in the situation of off-resonant driving in general. In particular, for the present many-body system, the off-resonant situation is realised when the photon energy ω is chosen below the Mott gap $\sim U$ but above the band width $\sim t_0$ of doped holes. Such an energy window indeed exists in the strong-coupling regime, $t_0 \ll U$. Thanks to this hierarchy in the energy scale, one can determine $\hat{\Lambda}(t)$ in a perturbative manner^{11,12,18,27,28}, as detailed in Methods. While the $t_0 \ll U$ assumption yields a low-energy effective model known in the undriven case as a t - J model²⁹ which describes the dynamics of holes in the background of localised spins, an essential difference in the Floquet states under CPL is that extra terms emerge. Namely, the Hamiltonian of the irradiated case reads

$$\begin{aligned} \hat{H}_F = & - \sum_{ij\sigma} \tilde{t}_{ij} \hat{P}_G \hat{c}_{i\sigma}^\dagger \hat{c}_{j\sigma} \hat{P}_G + \frac{1}{2} \sum_{ij} J_{ij} \left(\hat{\mathbf{S}}_i \cdot \hat{\mathbf{S}}_j - \frac{1}{4} \hat{n}_i \hat{n}_j \right) \\ & + \sum_{ijk\sigma\sigma'} \Gamma_{i,j;k} \hat{P}_G \left[(\hat{c}_{i\sigma}^\dagger \sigma_{\sigma\sigma'} \hat{c}_{j\sigma'}) \cdot \hat{\mathbf{S}}_k - \frac{1}{2} \delta_{\sigma\sigma'} \hat{c}_{i\sigma}^\dagger \hat{c}_{j\sigma} \hat{n}_k \right] \hat{P}_G \\ & + \frac{1}{6} \sum_{ijk} J_{ijk}^\chi (\hat{\mathbf{S}}_i \times \hat{\mathbf{S}}_j) \cdot \hat{\mathbf{S}}_k, \end{aligned} \quad (5)$$

where $\hat{P}_G = \prod_i (1 - \hat{n}_{i\uparrow} \hat{n}_{i\downarrow})$ projects out doubly-occupied configurations. Here, we have retained all the processes up to the second order (in the hopping amplitudes t_0, t'_0), and additionally taken account of the fourth-order processes for the last line of the above equation. Thus the photon-modified exchange interaction J_{ij} and the photon-induced correlated hopping $\Gamma_{i,j;k}$ are of second order, while the photon-generated chiral spin coupling J_{ijk}^χ is of fourth order.

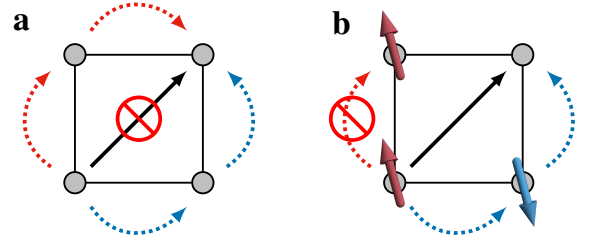


Fig. 2. **Schematic picture for two-step hopping.** **a** Photon-induced hopping processes in the noninteracting square lattice, where contributions from two different paths (red and blue dotted arrows) cancel with each other. **b** For a strongly-correlated model, the photon-induced hopping processes are sensitive to the charge and spin configurations on the path, which lifts the cancellation in general.

In the effective model in the presence of the laser field, first, the hopping amplitude of the holes is renormalised from t_{ij} into $\tilde{t}_{ij} = t_{ij} \mathcal{J}_0(A_{ij})$ due to the time-averaged Peierls phase^{30,31}, where $A_{ij} = ER_{ij}/\omega$ and \mathcal{J}_m is the m -th Bessel function. Second, as for the interaction, the spin-spin interaction, which is mediated by kinetic motion of electrons, has a coupling strength dramatically affected by the intense light field. Namely, the static kinetic-exchange interaction J is modulated as²⁷

$$J_{ij} = \sum_{m=-\infty}^{\infty} \frac{4t_{ij}^2 \mathcal{J}_m(A_{ij})^2}{U - m\omega}, \quad (6)$$

which is a sum over m -photon processes, and appears in the second term on the first line of Eq. (5).

While these modulations of t and J also occur for the case of linearly-polarised lasers (i.e., for time-reversal symmetric modulations), a notable feature of the CPL is the emergence of the *time-reversal breaking many-body interactions* specific to the strong correlation. The time-reversal breaking term is known to arise in the noninteracting honeycomb lattice as an imaginary two-step hopping process (i.e., a perturbative process with hopping twice), which plays a central role in the topological phase transition to the Floquet topological insulator^{2,6,8}. In the noninteracting square lattice, such an imaginary hopping does not arise due to a cancellation of contributions from different paths as depicted in Fig. 2a.

On the other hand, the hopping process in correlated systems involves interaction with the electrons on the path, which lifts such cancellations, as exemplified in Fig. 2b. Such a two-step correlated hopping Γ appears in the second-order perturbation in the presence of holes [the second line of Eq. (5)], which involves three sites and sometimes referred to as the “three-site term”²⁹. While the three-site term also appears in the undriven case with the amplitude $\Gamma_{i,j;k} = J_{ij}/4$, this term involving the dynamics of holes (the change of holes’ positions) is usually neglected because its contribution is small in the low-doping regime (see the Gutzwiller factor in the next subsection). In sharp contrast, when the system is driven by a

CPL, $\Gamma_{i,j,k}$ acquires an important *three-site imaginary part* as

$$\text{Im } \Gamma_{i,j,k} = \sum_{m=1}^{\infty} \frac{2t_{ik}t_{kj}\mathcal{J}_m(A_{ik})\mathcal{J}_m(A_{kj})}{m\omega(1-m^2\omega^2/U^2)} \sin m(\theta_{jk} - \theta_{ik}) \quad (7)$$

with θ_{ij} defined as $\mathbf{R}_{ij} = R_{ij}(\cos \theta_{ij}, \sin \theta_{ij})$. The term triggers a topological superconductivity even when it is small, as we shall see.

In addition to the two-step correlated hopping Γ , time-reversal breaking terms arise if we go over to higher-order perturbations. In the previous studies of the half-filled cases^{11,12}, an emergent three-spin interaction, the scalar *spin chirality term* J^χ , is shown to appear in the fourth-order perturbation. This appears on the last line in Eq. (5) with a coefficient J_{ijk}^χ . While this term is basically much smaller than the second-order terms, it may become comparable with the contribution from $\text{Im } \Gamma$, as the chirality term does not accompany the dynamics of holes and has a larger Gutzwiller factor.

B. Mean-field decomposition under Gutzwiller ansatz

Let us investigate the fate of the d -wave superconductivity in the presence of the time-reversal breaking terms. To this end, we here adopt the Gutzwiller ansatz^{29,32} for the ground-state wavefunction and perform a mean-field analysis, as detailed in Methods. After the approximate evaluation of the Gutzwiller projection, the problem to determine the ground state is turned into an energy minimisation of Eq. (5) without the Gutzwiller factor \hat{P}_G if we renormalise the parameters. The mean-field solution is then formulated as a diagonalisation of the Bogoliubov-de Gennes Hamiltonian in the momentum space,

$$\hat{H}_F = \sum_{\mathbf{k}} \begin{pmatrix} \hat{c}_{\mathbf{k}\uparrow} \\ \hat{c}_{-\mathbf{k}\downarrow}^\dagger \end{pmatrix}^\dagger \begin{pmatrix} \varepsilon(\mathbf{k}) & F(\mathbf{k}) \\ F(\mathbf{k})^* & -\varepsilon(-\mathbf{k}) \end{pmatrix} \begin{pmatrix} \hat{c}_{\mathbf{k}\uparrow} \\ \hat{c}_{-\mathbf{k}\downarrow}^\dagger \end{pmatrix} \quad (8)$$

$$= \sum_{\mathbf{k}} \begin{pmatrix} \hat{c}_{\mathbf{k}\uparrow} \\ \hat{c}_{-\mathbf{k}\downarrow}^\dagger \end{pmatrix}^\dagger \left[\sum_{\tau} \begin{pmatrix} \varepsilon_{\tau} & F_{\tau} \\ F_{\tau}^* & -\varepsilon_{\tau} \end{pmatrix} \cos \mathbf{k} \cdot \mathbf{R}_{i,i+\tau} \right] \begin{pmatrix} \hat{c}_{\mathbf{k}\uparrow} \\ \hat{c}_{-\mathbf{k}\downarrow}^\dagger \end{pmatrix}, \quad (9)$$

where

$$\begin{aligned} \varepsilon_{\tau} &= -g\delta\tilde{t}_{i,i+\tau} - g^2\frac{3-\delta^2}{8}J_{i,i+\tau}\chi_{\tau} \\ &- g^2\delta\sum_{\tau'} \text{Re} \left(\frac{1-\delta^2}{4}\Gamma_{i,i+\tau,i+\tau'} + \frac{3-\delta}{2}\Gamma_{i,i+\tau+\tau',i+\tau}\chi_{\tau'} \right) \\ &- \frac{3}{16}g^3\sum_{\tau'} J_{i,i+\tau,i+\tau'}^\chi \text{Im}(\Delta_{\tau+\tau'}^*\Delta_{\tau'}), \end{aligned} \quad (10)$$

$$\begin{aligned} F_{\tau} &= g^2\frac{3+\delta^2}{8}J_{i,i+\tau}\Delta_{\tau} + g^2\delta\frac{3+\delta}{2}\sum_{\tau'} \text{Re}\Gamma_{i,i+\tau+\tau',i+\tau}\Delta_{\tau'} \\ &+ ig^2\sum_{\tau'} \left(\delta\frac{3+\delta}{2}\text{Im}\Gamma_{i,i+\tau+\tau',i+\tau} + \frac{3}{8}gJ_{\chi,i,i+\tau,i+\tau+\tau'}\chi_{\tau+\tau'} \right) \Delta_{\tau'}, \end{aligned} \quad (11)$$

For the detailed derivation, see Methods. Here, the dependence on the doping level $\delta = 1 - \sum_i \langle \hat{n}_i \rangle / N$ and $g = 2/(1 + \delta)$

appears as a result of the Gutzwiller projection, which suppresses the contribution from charge dynamics as represented by \tilde{t} and Γ in the small δ regime (N is the number of lattice sites). Throughout the present study, we take $\delta = 0.2$. The mean-field Hamiltonian is self-consistently determined for the bond order parameter χ and the pairing amplitude Δ as

$$\chi_{\tau} = \frac{1}{N} \sum_i \langle \hat{c}_{i\uparrow}^\dagger \hat{c}_{i+\tau\uparrow} + \hat{c}_{i\downarrow}^\dagger \hat{c}_{i+\tau\downarrow} \rangle, \quad (12)$$

$$\Delta_{\tau} = \frac{1}{N} \sum_i \langle \hat{c}_{i\uparrow} \hat{c}_{i+\tau\downarrow} - \hat{c}_{i\downarrow} \hat{c}_{i+\tau\uparrow} \rangle. \quad (13)$$

In the absence of the external field, the system undergoes the phase transition to the $d_{x^2-y^2}$ -wave superconductivity when the temperature is sufficiently low²⁹. The corresponding order parameter is

$$\Delta_{\pm x} = -\Delta_{\pm y} \equiv \Delta, \quad (14)$$

for which the gap function becomes

$$F^{x^2-y^2}(\mathbf{k}) = \frac{3}{4}g^2J\Delta(\cos k_x - \cos k_y) \quad (15)$$

(with a small correction due to δ dropped here). Without a loss of generality, we assume that Δ is real. The $d_{x^2-y^2}$ gap function has nodal lines along $k_y = \pm k_x$, across which the gap function changes sign [See Figs. 4a-4c below].

Now let us look into the possibility for the laser field to convert this ground state into *topological superconductivity* from the time-reversal breaking terms [the second line in Eq. (11)]. The leading term should be those for $\tau' = \pm x, \pm y$ (i.e., $\Delta_{\tau'} = \pm\Delta$), which results in an imaginary gap function $\propto i\Delta$. In particular, gathering the terms with $\tau = \pm(x+y), \pm(x-y)$, we obtain the leading modulation to the gap function as

$$\delta F^{xy}(\mathbf{k}) = 3ig^2 \left[4\delta\gamma + g(J_{\chi}\chi_x + J'_{\chi}\chi_{2x+y}) \right] \Delta \sin k_x \sin k_y \quad (16)$$

with the two-step correlated hopping

$$\gamma = \text{Im}(\Gamma_{i-x,i,i+y} - \Gamma_{i-x-y,i+x,i}), \quad (17)$$

and the chiral spin-coupling

$$J_{\chi} = J_{i,i+y,i+x}^{\chi}, \quad J'_{\chi} = J_{i-x,i,i+x+y}^{\chi}. \quad (18)$$

Thus we are indeed led to an emergence of a topological (chiral) $d_{x^2-y^2} + id_{xy}$ superconductivity with $F(\mathbf{k}) \simeq F^{x^2-y^2} + i\delta F^{xy}$ with a full gap. For the full expression for the modulated gap function, see Eq. (62) in Methods. The key interactions, γ and J_{χ} , take nonzero values when the original Hubbard Hamiltonian Eq. (1) has the second-neighbour hopping t'_0 : Since the two-step correlated hopping $\Gamma_{i,j,k}$ is composed of two hoppings, $k \rightarrow i$ and $j \rightarrow k$, we can see that the imaginary coefficient above has $\gamma \propto t_0 t'_0$. The chiral spin-coupling $J_{\chi} \propto (t_0 t'_0)^2$ also necessitates the next-nearest-neighbour hopping, which can be deduced from Eq. (40) in Methods.

Having revealed the essential coupling for the chiral superconductivity, let us now explore how we can *optimise* the field

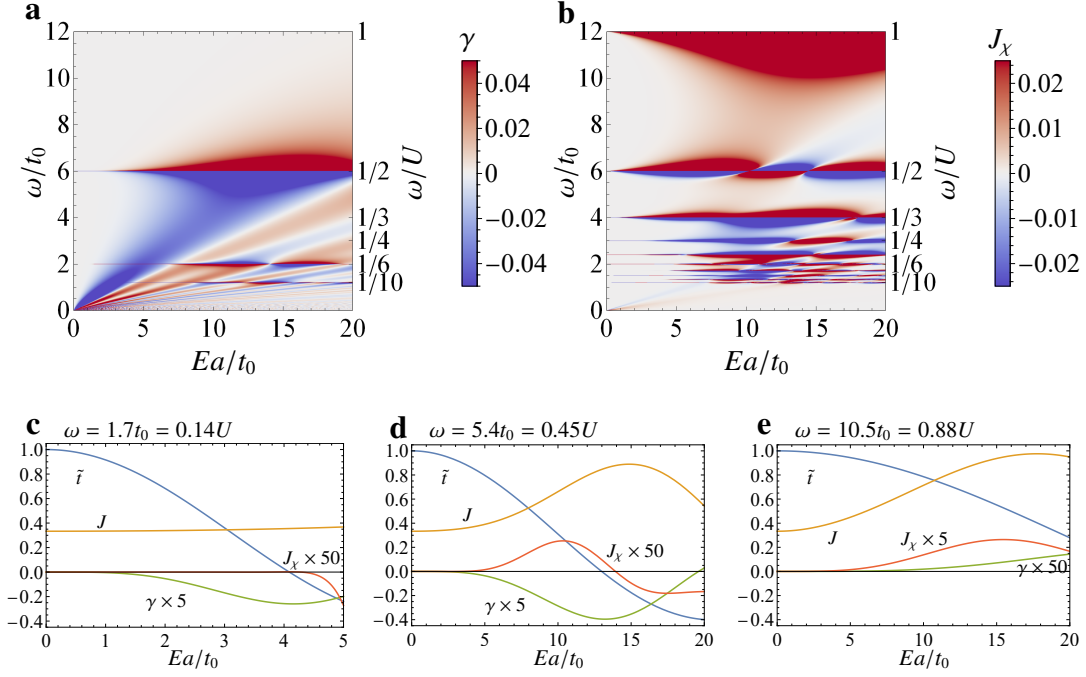


Fig. 3. **Dependence of the coupling constants on the laser intensity for the driven model.** **a, b** Two-step correlated hopping γ (**a**), and scalar spin-chirality term J_χ (**b**) against circularly-polarised-light amplitude E and driving frequency ω . Fig. 1d depicts a cross section of **b** at $E = 6t_0/a$. **c-e** The renormalised hopping amplitude for holes \tilde{t} , exchange coupling J , along with the two-step correlated hopping γ and the chiral spin-coupling J_χ , against E . The driving frequency is chosen as $\omega = 1.7t_0 = 0.14U$ (**c**), $\omega = 5.4t_0 = 0.45U$ (**d**), or $\omega = 10.5t_0 = 0.88U$ (**e**) with t_0 : bare hopping amplitude, a : lattice constant. Note a difference in the horizontal scale in **a**. We take here the bare second-neighbour hopping $t'_0 = -0.2t_0$, the onsite interaction $U = 12t_0$, and a doping level $\delta = 0.2$.

amplitude and frequency for realising larger topological gaps. For this, we set here $t'_0 = -0.2t_0$ and $U = 12t_0$ with cuprates having $t_0 \approx 0.4$ eV in mind as a typical example.

We plot the essential γ and J_χ against the driving amplitude E and frequency ω in Figs. 3a and 3b. We have here truncated the summation of Fourier components at $O(E^{21})$, so that the intricate structure in the low-frequency regime ($\omega \lesssim t_0$) is not fully captured, which is outside the present interest and the regime for the present method to be reliable. If we look at the overall picture, we can see that the dynamical time-reversal breaking is strongly enhanced along some characteristic frequencies in a *resonant* fashion, which we can capture from the expressions for the coupling constants in the small-amplitude regime as follows.

The expression for γ in the leading order in the amplitude is

$$\gamma = \frac{2t_0 t'_0 \mathcal{J}_2\left(\frac{Ea}{\omega}\right) \mathcal{J}_2\left(\sqrt{2}\frac{Ea}{\omega}\right)}{\omega(1 - 4\omega^2/U^2)} + O(E^{12}). \quad (19)$$

This expression, as a function of E , takes the maximal value around $E \approx 2.45\omega/a$, while diverges for $\omega \rightarrow 0$ or $\omega \rightarrow U/2$ for each value of E , as seen from the energy denominator. The enhancement occurs even in the low-frequency regime, which should be advantageous for experimental feasibility, since the required field amplitude ($E \approx 2.4\omega/a$) can be small.

If we turn to the spin-chirality term, J_χ has a complicated form involving Bessel functions [See Eq. (40)]. If we Taylor-

expand with respect to E , we have

$$J_\chi \sim \frac{2(Ea)^4 t_0'^2 t_0'^2 (2U^6 + 75\omega^2 U^4 - 399\omega^4 U^2 - 164\omega^6)}{\omega(U^2 - \omega^2)^3 (U^2 - 4\omega^2)^3}, \quad (20)$$

which takes large values around $\omega = U$ due to the energy denominator in the above expression, while γ is small in this regime. The expression reveals that a dynamical time-reversal breaking occurs as a fourth-order nonlinear effect with respect to the field strength E as well.

Let us look in Figs. 3c-e at how J_χ , as well as the exchange interaction J and the time-averaged hopping amplitude for nearest neighbours \tilde{t} , vary with the field intensity for several representative frequencies where the dynamical time reversal breaking becomes prominent. The hopping amplitude \tilde{t} decreases to vanish around the peak of γ ($E \approx 2.45\omega/a$), as seen in Figs. 3c,d. This involves the zero of the Bessel function (at $E \sim 2.40\omega/a$), and known as the dynamical localisation³⁰. In Figs. 3d and 3e, we can see a strong enhancement of J . Panel d has $\omega = 0.45U$ (slightly red-detuned from $U/2$), while panel e has $\omega = 0.88U$ (slightly red-detuned from U). If we go back to Eq. (6), the former has to do with the energy denominator for $m = 2$, while the latter for $m = 1$. While the driving frequency is set to be red-detuned from the “ $U - m\omega$ resonance” in these cases, we obtain negative contributions from these terms if we make them blue-detuned, where the negative terms leading to a ferromagnetic exchange interaction

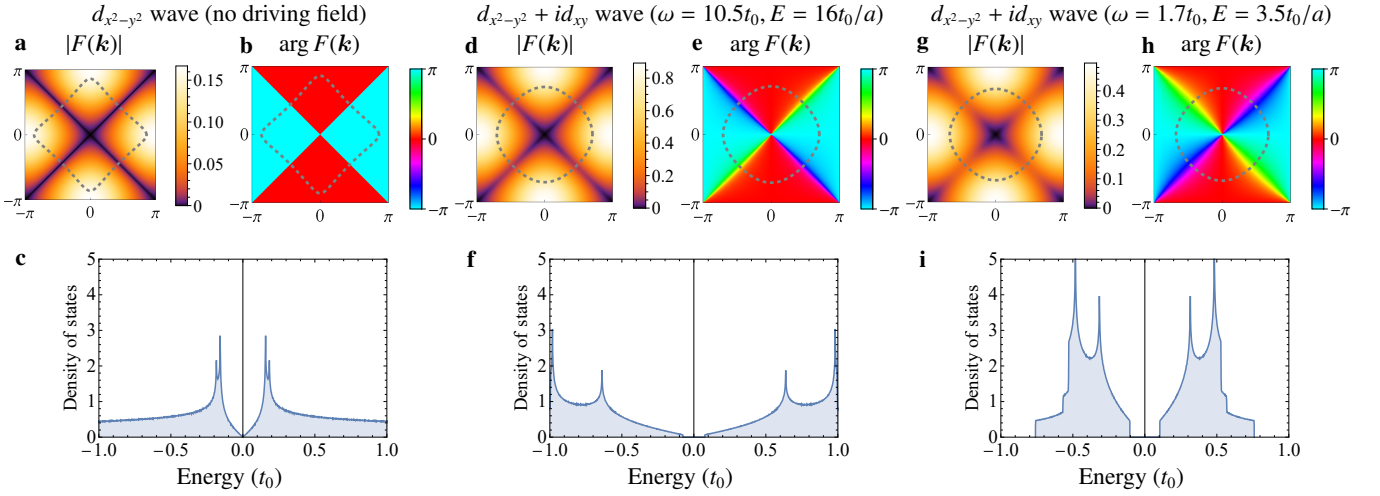


Fig. 4. **Gap functions.** **a,d,g** Absolute values of the gap function, $|F(\mathbf{k})|$. **b,e,h** Phases, $\arg F(\mathbf{k})$. The dashed lines represent the Fermi surface at the critical temperature $T = T_c$. **c,f,i** Density of states against energy in units of the bare hopping amplitude t_0 . **a-c** $d_{x^2-y^2}$ -wave superconductivity in the absence of driving field. **d-i** $d_{x^2-y^2} + id_{xy}$ -wave superconductivity in the circularly-polarised laser light, where the driving frequency ω and the field amplitude E are chosen as $\omega = 10.5t_0 = 0.88U$, $E = 16t_0/a$ (**d-f**), and $\omega = 1.7t_0 = 0.14U$, $E = 3.5t_0/a$ (**g-i**). The bare second-neighbour hopping is $t'_0 = -0.2t_0$, the onsite interaction $U = 12t_0$, and a doping level $\delta = 0.2$.

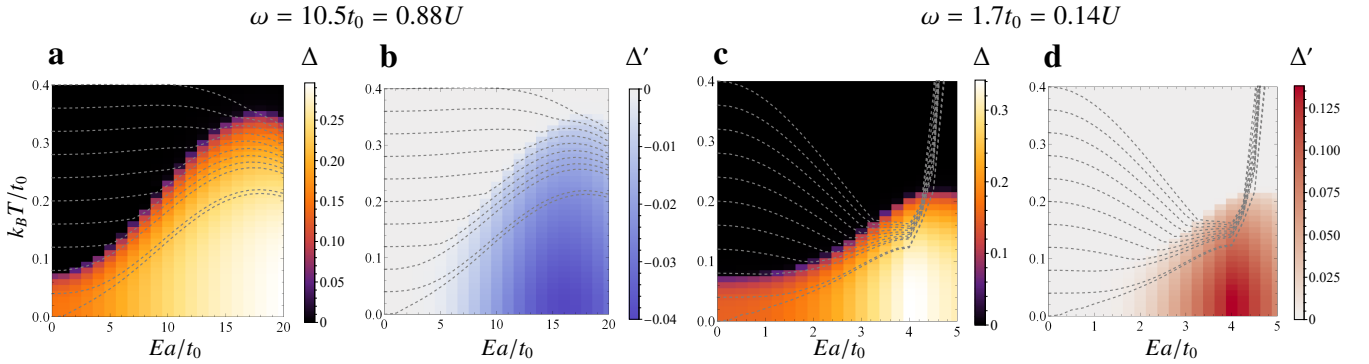


Fig. 5. **Finite-temperature phase diagram.** The superconducting order parameter $|\Delta|$ (**a, c**) and the time-reversal breaking order parameter $\Delta' \equiv -i\Delta_{\pm(x+y)} = i\Delta_{\pm(x-y)}$ (**b, d**) plotted against the field amplitude E and temperature T . The driving frequency is set to $\omega = 10.5t_0 = 0.88U$ (**a, b**) or $\omega = 1.7t_0 = 0.14U$ (**c, d**). Dotted lines represent the effective temperature of the Floquet Hamiltonian when the system is quenched from $E = 0$ at a temperature that is the leftmost starting point of each dotted line. The bare second-neighbour hopping is $t'_0 = -0.2t_0$, the onsite interaction $U = 12t_0$, and a doping level $\delta = 0.2$.

would unfavour the d -wave superconductivity. With an optimal choice of the driving field, γ attains a significantly large value $\approx 0.04t_0$, which yields $\delta F^{xy}(\mathbf{k}) \approx 0.3t_0 \times i\Delta \sin k_x \sin k_y$ (for $\delta = 0.2$). This is remarkably large for the gap function in the absence of laser $F^{x^2-y^2}(\mathbf{k}) \approx 0.7t_0 \times \Delta(\cos k_x - \cos k_y)$, even though the coupling constant itself is much smaller than J . This is the first key result of the present work.

C. Phase diagram

Now we investigate the ground state of the effective static Bogoliubov-de Gennes Hamiltonian for several choices of the field parameters. We show the gap function and the density of states in Fig. 4. In the absence of the external field in

Figs. 4a-4c, the gap function has the $d_{x^2-y^2}$ symmetry with nodal lines that gives the zero gap at the Fermi energy. Now we turn on the CPL, with $\omega = 10.5t_0 = 0.88U$, $E = 16t_0/a$ for Figs. 4d-4f, and with $\omega = 1.7t_0 = 0.14U$, $E = 3.5t_0/a$ for Figs. 4g-4i. The former represents the case where J_χ is dominant (see Fig. 3e), while γ plays the central role in the latter. In both cases we have the $d_{x^2-y^2} + id_{xy}$ symmetry of the gap function, where the nodal lines are gapped out due to the complex amplitudes. We can indeed see clear energy gaps in the density of states with a gap size comparable with the original $d_{x^2-y^2}$ superconducting gap (as measured by the energy spacing between the two peaks in the density of states). The band width and the $d_{x^2-y^2}$ superconducting gap are renormalised there, due to the change in \tilde{t} and J .

To examine the robustness of the $d + id$ superconductivity,

we calculate Δ and $\Delta' \equiv -i\Delta_{\pm(x+y)} = i\Delta_{\pm(x-y)}$ at finite temperatures, which gives a phase diagram against field amplitude E in Fig. 5. We can see that the critical temperature T_c , as delineated by the region for $\Delta \neq 0$, increases significantly as the field amplitude E is increased. This is originated from the fact that J [and $\text{Re } \Gamma$, see Eq. (37) below] are enhanced when the laser is applied, as we have seen in Figs. 3c-3e. The time-reversal breaking order parameter Δ' emerges below T_c down to $T = 0$, with the field dependence emerging from that of γ and J_χ .

D. Transient dynamics

So far, we have investigated static properties of the effective Hamiltonian \hat{H}_F in the Floquet formalism. While the results clearly show the presence of Floquet topological superconductivity in a wide parameter region, an important question from a dynamical viewpoint is whether we can achieve the Floquet topological superconductivity within a short enough time scale, over which the description with the effective Hamiltonian Eq. (5) is valid (i.e., over which we can neglect the heating process towards the infinite temperature, coupling to phonons, etc).

Thus let us study the dynamics of the superconducting gap, by solving a quench problem formulated as follows. We first prepare the initial state as the mean-field ground state of the equilibrium t - J model [i.e., Eq. (5) with $E = 0$], and then look at the transient dynamics when the CPL electric field is suddenly switched on, by changing the Hamiltonian at $t = 0$ to the effective Hamiltonian \hat{H}_F (5) with $E \neq 0$. In such a treatment, $\langle \hat{H}_F \rangle$ is a conserved quantity for $t > 0$, and the driven state is expected to thermalise to the equilibrium state of \hat{H}_F with the temperature that corresponds to the internal energy $\langle \hat{H}_F \rangle$.

Before exploring the dynamics, it is important to check whether the expected steady state of the quench problem remains superconducting. We show the effective temperature defined above, as indicated by dotted lines in Fig. 5. While the effective temperature rises as we increase the field strength E when we start from the zero-temperature state, we can see that the effective temperature does *not* exceed T_c in a wide parameter region, which implies that the Floquet topological superconductivity should indeed appear as a steady state of the quench dynamics. A sudden increase of temperature around $E \sim 4t_0/a$ in Figs. 5c, 5d is due to the band flipping (sign change of \hat{t}), which makes the kinetic energy of the initial state quite large. As we further increase the field strength, the effective temperature eventually reaches infinity and will even become negative¹³.

Now, the problem is whether the equilibration (known as the Floquet prethermalisation) occurs fast enough (e.g., faster than the heating towards the infinite temperature, within the experimentally accessible pulse duration, etc.). We compute the time evolution of the superconducting order parameter in the time-dependent mean-field approximation (with the Gutzwiller ansatz), and plot the time evolution of $|\Delta|$ and $|\Delta'|$ in Figs. 6a, 6b, where we set the initial temperature at

$k_B T_{\text{initial}} = 0$ with $E = 7t_0/a$, $\omega = 10.5t_0 = 0.88U$. Here, the unit of time \hbar/t_0 corresponds to ~ 1 fs for $t \simeq 0.4$ eV. $|\Delta|$ rapidly evolves with an overshooting behaviour, and converges to a certain value with a damped oscillation. Similar behaviour can be found in a previous study of the quench problem for the d -wave (but within the $d_{x^2-y^2}$ pairing) superconductor³³. Along with this, the time-reversal breaking order parameter $|\Delta'|$ also quickly converges to a nonzero value. We note that the obtained steady state slightly deviates from the equilibrium state with respect to \hat{H}_F , which arises because of the lack of the pair-breaking scattering³³ in the mean-field treatment of the dynamics.

The curious oscillation in the amplitude of the gap function can be interpreted as excitation of the *Higgs modes* in superconductors³⁴⁻³⁶, and thus the typical time scale for the oscillation (and the emergence of Δ') can be roughly estimated as the inverse of the superconducting gap $\sim 1/2|F(\mathbf{k})|$ (with an appropriate k -average). We can analyse the present quench dynamics in a linearised form³⁷ if the change in the coupling constant is small, which reveals that the appearance of Δ' is described as the A_{2g} Higgs mode with an amplitude proportional to E^4 .

If we have a closer look at the effective temperature in Fig. 5, we find an intriguing phenomenon: the superconducting state can appear even when we start from an initial temperature that is above T_c . Namely, some dotted lines that start from T above T_c at $E = 0$ do plunge into the superconducting region as E is increased. We show the time evolution of the order parameter for this “nonequilibrium-induced superconductivity” in Figs. 6c, 6d, where we set $k_B T_{\text{initial}} = 0.2t_0$ as an initial temperature, and choose $E = 16t_0/a$, $\omega = 10.5t_0$. Since the homogeneous mean-field ansatz without fluctuation cannot describe the spontaneous symmetry breaking, we instead inspect the growth of a tiny (homogeneous) perturbation $\Delta = 10^{-4}$ on the initial state. After the quench, both of the gap functions Δ and Δ' grow exponentially and converge respectively to nonzero values, although the damped oscillation is slower than the previous case, and the converged values are far below those expected for equilibrium with the effective temperature, $|\Delta| \simeq 0.18$ and $|\Delta'| \simeq 0.03$.

III. DISCUSSION

In the present paper we show that Floquet-induced interactions does indeed give rise to topological superconductivity. The phenomenon revealed here can provide a novel way to induce a topological superconductivity.

Let us recapitulate advantages of the present proposal for the Floquet topological superconductivity. In the previous study of Floquet topological superconductivity in cuprates¹⁶, the topological transition is triggered by the modulation of the kinetic part of the Hamiltonian [diagonal components in Eq. (8)], while the pairing symmetry of the gap function remains the same. The nontrivial structure of the kinetic part necessitates the presence of strong Rashba spin-orbit coupling, which would limit the applicable class of materials. In the present approach, by contrast, we exploit the correlation ef-

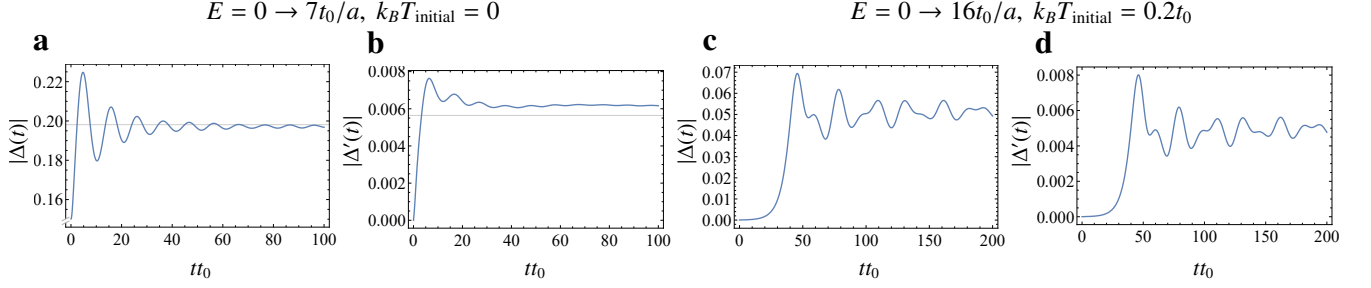


Fig. 6. **Quench dynamics of order parameters.** Time evolution of $|\Delta| = |\langle c_{i\uparrow} c_{i+x,\downarrow} \rangle|$ (a, c), and $|\Delta'| = |\langle c_{i\uparrow} c_{i+x+y,\downarrow} \rangle|$ (b, d) after a sudden quench of the field amplitude from $E = 0$ to $E = 7t_0/a$ with an initial temperature $k_B T_{\text{initial}} = 0$ (a, b), or to $E = 16t_0/a$ with an initial $k_B T_{\text{initial}} = 0.2t_0$ (c, d). The latter correspond to the case in which the superconductivity appears even when we start from an initial temperature above T_c . Horizontal lines indicate the equilibrium value at the effective temperature. The driving frequency is set to $\omega = 10.5t_0 = 0.88U$ with t_0 being the bare hopping amplitude.

fects themselves, with which we can directly modulate the pairing symmetry to obtain the topological superconductivity. Our approach does not require nontrivial structures in the one-body part, either, and thus a simple square lattice Hubbard model suffices for inducing topological transition.

While the emergence of the topological superconductivity is verified here with a numerically economical approach, it is an important future problem to examine this with more sophisticated methods. Of particular importance is an elaboration of the heating process neglected in the present effective static approach, by, e.g., analysing a time-dependent problem. While we have evoked the enhancement of γ and J_χ near the resonance, we have technically a trade-off between the resonance-originated enhancement and the accuracy of the asymptotic expansion, where the heating (embedded in the truncation error) is expected to be faster as we approach the resonance. Thus, whether the time scale $t \sim 10/t_0$ for the emergence of Δ' (See Fig. 6b) lies within the validity of the static description should be addressed. On the other hand, since the effective Hamiltonian with the time-reversal breaking is obtained by fully taking account of the noncommutative nature of the Gutzwiller projector \hat{P}_G (whereas the usual hopping terms are commutative), it should be important to include relevant correlation effects when performing such a dynamical simulation. As for nonequilibrium modifications of superconductivity, there is existing literature that reports such phenomena³⁸ along with related theories^{39–42}. Whether the present theory has some possible relevance will be a future problem.

Let us turn to the required field amplitude and frequency for the experimental feasibility. Specifically when we want to employ the enhancement of time-reversal breaking around $\omega = U/2$ or U , the required field intensity is $E \sim 10t_0/a$, which corresponds to $E \sim 10^2$ MV/cm for the typical cuprates with $t_0 \simeq 0.4$ eV, $a \simeq 3\text{\AA}$. One reason why the strong intensities are required derives from the fact that the time-reversal breaking terms evoked here are of fourth order in E , while usually the time-reversal breaking terms can be of second order^{11,12}. This comes from the cancellation similar to Fig. 2a for the present square lattice, but this can be avoided in e.g. hexagonal lattices (such as honeycomb and kagome). So the application of the present mechanism for the Floquet topo-

logical superconductivity to a wider class of materials with various lattice structures and/or multi-orbitals may be an interesting strategy. More trivially, as the required intensity scales with the frequency ω , going to low frequencies is another practical route for the enhanced γ . A possibility of chiral superconductivity triggered by the same interaction but with a different mechanism (such as proposed for the doped spin liquid on triangular lattice⁴³) is also of interest.

We can further raise an intriguing possibility that, since the emergence of the topological superconductivity is intimately related to the excitation of Higgs modes as mentioned above, the topological signature might be enhanced by resonantly exciting the Higgs modes, which provides another future problem.

METHODS

1. Time-periodic Schrieffer-Wolff transformation

To obtain the effective low-energy Hamiltonian in the presence of the laser electric field, we employ the time-periodic Schrieffer-Wolff transformation (canonical transformation). Following the previous study¹¹ (but extending it for the case where holes exist. See also Ref.¹⁸), we decompose the Hubbard Hamiltonian as

$$\hat{H}(t) = -\lambda \sum_{m=-\infty}^{\infty} (\hat{T}_{-1,m} + \hat{T}_{0,m} + \hat{T}_{+1,m}) e^{-im\omega t} + U\hat{D}, \quad (21)$$

where λ is a bookkeeping parameter, which bridges the atomic limit $\lambda = 0$ to the system of interest $\lambda = 1$, and $\hat{D} = \sum_i \hat{n}_{i\uparrow} \hat{n}_{i\downarrow}$ counts the number of doubly-occupied sites. The hopping operator $\hat{T}_{+d,m}$ increases the number of doubly-occupied sites by

+d, as given by

$$\hat{T}_{0,m} = \sum_{ij\sigma} t_{ij}^{(m)} \left[\hat{n}_{i\bar{\sigma}} \hat{c}_{i\sigma}^\dagger \hat{c}_{j\sigma} \hat{n}_{j\bar{\sigma}} + (1 - \hat{n}_{i\bar{\sigma}}) \hat{c}_{i\sigma}^\dagger \hat{c}_{j\sigma} (1 - \hat{n}_{j\bar{\sigma}}) \right], \quad (22)$$

$$\hat{T}_{+1,m} = \sum_{ij\sigma} t_{ij}^{(m)} \hat{n}_{i\bar{\sigma}} \hat{c}_{i\sigma}^\dagger \hat{c}_{j\sigma} (1 - \hat{n}_{j\bar{\sigma}}) = \hat{T}_{-1,-m}^\dagger, \quad (23)$$

$$t_{ij}^{(m)} = t_{ij} \frac{\omega}{2\pi} \int_0^{2\pi/\omega} dt e^{-i\mathbf{A}(t) \cdot \mathbf{R}_{ij} + im\omega t} \quad (24)$$

$$= t_{ij} \mathcal{J}_m(A_{ij}) (-1)^m e^{im\theta_{ij}}, \quad (25)$$

where $\bar{\sigma} \equiv -\sigma$. We also decompose the generator $\hat{\Lambda}(t)$ in Eq. (4) into $e^{i\hat{\Lambda}(t)} = e^{i\hat{\Lambda}_h(t)} e^{i\hat{\Lambda}_c(t)}$, where $\hat{\Lambda}_c$ eliminates the charge excitation that creates doubly-occupied sites from the transformed Hamiltonian, while $\hat{\Lambda}_h$ makes the Hamiltonian static.

We first consider $\hat{H}_c(t) := \hat{P}_G e^{i\hat{\Lambda}_c(t)} (\hat{H}(t) - i\partial_t) e^{-i\hat{\Lambda}_c(t)} \hat{P}_G$. Let us introduce a series solution,

$$\hat{\Lambda}_c(t) = \sum_{n=1}^{\infty} \sum_{d \neq 0} \sum_{m=-\infty}^{\infty} \lambda^n \hat{\Lambda}_{+d,m}^{(n)} e^{-im\omega t} \quad (26)$$

with $[\hat{D}, \hat{\Lambda}_{+d,m}^{(n)}] = d\hat{\Lambda}_{+d,m}^{(n)}$, which eliminates the charge excitation from $\hat{H}_c(t)$, i.e., $[\hat{D}, e^{i\hat{\Lambda}_c(t)} (\hat{H}(t) - i\partial_t) e^{-i\hat{\Lambda}_c(t)}] = 0$. The form of $\hat{\Lambda}_{+d,m}^{(n)}$ can be uniquely determined order by order, and we arrive at

$$\begin{aligned} \hat{H}_c &= -\lambda \sum_{m=-\infty}^{\infty} \hat{P}_G \hat{T}_{0,m} \hat{P}_G e^{-im\omega t} \\ &+ \lambda^2 \sum_{n,m=-\infty}^{\infty} \frac{\hat{P}_G [\hat{T}_{+1,n}, \hat{T}_{-1,m-n}] \hat{P}_G}{2(U - n\omega)} e^{-im\omega t} + \text{H.c.} + O(\lambda^3). \end{aligned} \quad (27)$$

While this Hamiltonian projected onto the spin subspace is evaluated in the previous study, here we need to consider the expression for nonzero numbers of holes. We then obtain

$$\begin{aligned} &\hat{P}_G [\hat{T}_{+1,n}, \hat{T}_{-1,m-n}] \hat{P}_G \\ &= - \sum_{ijk\sigma\sigma'} \hat{P}_G (t_{ij}^{(m-n)} \hat{c}_{i\sigma}^\dagger \hat{c}_{j\sigma} \hat{n}_{j\bar{\sigma}} (t_{jk}^{(n)} \hat{c}_{j\sigma'}^\dagger \hat{c}_{k\sigma'})) \hat{P}_G \\ &= \sum_{ijk\sigma\sigma'} t_{ij}^{(m-n)} t_{jk}^{(n)} \hat{P}_G \left[(\hat{c}_{i\sigma}^\dagger \sigma_{\sigma\sigma'} \hat{c}_{k\sigma'}) \cdot \hat{\mathbf{S}}_j - \frac{1}{2} \delta_{\sigma\sigma'} \hat{c}_{i\sigma}^\dagger \hat{c}_{k\sigma'} \hat{n}_j \right] \hat{P}_G. \end{aligned} \quad (29)$$

Note that, while we recover the Heisenberg interaction for $k = i$, the terms with $k \neq i$ are so-called *three-site terms*. The final static Hamiltonian $\hat{H}_F = e^{i\hat{\Lambda}_h(t)} (\hat{H}_c - i\partial_t) e^{-i\hat{\Lambda}_h(t)}$ is obtained by using the formula^{8,11,23}

$$\hat{H}_F = \hat{H}_{c,0} + \sum_{m \neq 0} \frac{[\hat{H}_{c,-m}, \hat{H}_{c,m}]}{2m\omega} + O(\omega^{-2}), \quad (30)$$

where $\hat{H}_{c,m} \equiv (\omega/2\pi) \int_0^{2\pi/\omega} dt \hat{H}_c e^{im\omega t}$. The second term is

calculated up to λ^2 as

$$\sum_{m \neq 0} \frac{[\hat{H}_{c,-m}, \hat{H}_{c,m}]}{2m\omega} = \lambda^2 \sum_{m \neq 0} \frac{\hat{P}_G [\hat{T}_{0,-m}, \hat{T}_{0,m}] \hat{P}_G}{2m\omega} \quad (31)$$

$$\begin{aligned} &= \lambda^2 \sum_{ijk\sigma\sigma'} \sum_{m \neq 0} \frac{t_{ij}^{(-m)} t_{jk}^{(m)}}{m\omega} \\ &\times \hat{P}_G \left[(\hat{c}_{i\sigma}^\dagger \sigma_{\sigma\sigma'} \hat{c}_{k\sigma'}) \cdot \hat{\mathbf{S}}_j + \delta_{\sigma\sigma'} \hat{c}_{i\sigma}^\dagger \hat{c}_{k\sigma'} \frac{2 - \hat{n}_j}{2} \right] \hat{P}_G, \end{aligned} \quad (32)$$

where we have used $\{\hat{c}_{i\sigma}(1 - \hat{n}_{i\bar{\sigma}}), (1 - \hat{n}_{j\bar{\sigma}}) \hat{c}_{j\sigma'}^\dagger\} = \delta_{ij} [\delta_{\sigma\sigma'} (1 - \hat{n}_i/2) + \sigma_{\sigma\sigma'} \cdot \hat{\mathbf{S}}_i]$, $\{(1 - \hat{n}_{i\bar{\sigma}}) \hat{c}_{i\sigma}^\dagger, (1 - \hat{n}_{j\bar{\sigma}}) \hat{c}_{j\sigma'}^\dagger\} = 0$.

The effective Hamiltonian Eq. (4) is obtained up to the second order as

$$\begin{aligned} \hat{H}_F &= - \sum_{ij\sigma} \tilde{t}_{ij} \hat{P}_G \hat{c}_{i\sigma}^\dagger \hat{c}_{j\sigma} \hat{P}_G + \frac{1}{2} \sum_{ij} J_{ij} \left(\hat{\mathbf{S}}_i \cdot \hat{\mathbf{S}}_j - \frac{1}{4} \hat{n}_i \hat{n}_j \right) \\ &+ \sum_{ijk\sigma\sigma'} \Gamma_{i,j;k} \hat{P}_G \left[(\hat{c}_{i\sigma}^\dagger \sigma_{\sigma\sigma'} \hat{c}_{k\sigma'}) \cdot \hat{\mathbf{S}}_k - \frac{1}{2} \delta_{\sigma\sigma'} \hat{c}_{i\sigma}^\dagger \hat{c}_{k\sigma'} \hat{n}_k \right] \hat{P}_G, \end{aligned} \quad (33)$$

where

$$\tilde{t}_{ij} = t_{ij}^{(0)} - \sum_k \sum_{m \neq 0} \frac{t_{ik}^{(-m)} t_{kj}^{(m)}}{m\omega}, \quad (34)$$

$$J_{ij} = \sum_{m=-\infty}^{\infty} \frac{4U |t_{ij}^{(m)}|^2}{U^2 - m^2 \omega^2}, \quad (35)$$

$$\Gamma_{i,j;k} = \left[\frac{t_{ik}^{(0)} t_{kj}^{(0)}}{U} + \sum_{m \neq 0} \frac{t_{ik}^{(-m)} t_{kj}^{(m)}}{m\omega(1 - m\omega/U)} \right] (1 - \delta_{ij}). \quad (36)$$

Note that the second term in the hopping \tilde{t}_{ij} describing the two-step hopping vanishes for the square lattice [See Fig. 2(a)], and the renormalised hopping is given as $\tilde{t}_{ij} = t_{ij}^{(0)} = t_{ij} \mathcal{J}_0(A_{ij})$ if we put $m = 0$ in Eq. (25). For the Heisenberg term J_{ij} we end up with Eq. (6) in the main text. The two-step correlated hopping is much more intricate, and reads

$$\begin{aligned} \Gamma_{i,j;k} &= \frac{t_{ik} t_{kj} \mathcal{J}_0(A_{ik}) \mathcal{J}_0(A_{kj})}{U} \\ &+ \sum_{m \neq 0} \frac{t_{ik} t_{kj} \mathcal{J}_m(A_{ik}) \mathcal{J}_m(A_{kj})}{m\omega(1 - m\omega/U)} e^{im(\theta_{jk} - \theta_{ik})}. \end{aligned} \quad (37)$$

In the main text, we have also considered the scalar spin-chirality term J_{ijk}^χ , which appears in the fourth-order perturbation. While the perturbative processes involving three sites are considered in the previous studies^{11,12}, we need to evaluate the processes involving four sites as well for the present case of the square lattice. By dropping the density dependent part, $\hat{\mathbf{S}}_i \cdot (\hat{\mathbf{S}}_j \times \hat{\mathbf{S}}_k) (1 - \hat{n}_h) \sim O(\delta)$, we obtain

$$J_{ijk}^\chi = 2\text{Im} \sum_{lmn=-\infty}^{\infty} (K_{ijk}^{lmn} + K_{jki}^{lmn} + K_{kij}^{lmn} - K_{jik}^{lmn} - K_{kji}^{lmn} - K_{ikj}^{lmn}), \quad (38)$$

where

$$\begin{aligned}
K_{ijk}^{lmn} = & \frac{2t_{ij}^{(-l-m)}t_{ji}^{(l-m)}t_{jk}^{(m-n)}t_{kj}^{(n+m)}(1-\delta_{m,0})}{m\omega[U+(l-m)\omega][U-(n+m)\omega]} \\
& - \frac{2t_{ij}^{(m-n)}t_{ji}^{(l)}t_{jk}^{(n)}t_{kj}^{(-l-m)}}{(U+l\omega)(U-m\omega)(U-n\omega)} \\
& - \sum_{h \neq ijk} \frac{t_{ij}^{(-l-m)}t_{jk}^{(l)}t_{kh}^{(m-n)}t_{hi}^{(n)} + t_{ij}^{(m-n)}t_{jk}^{(l)}t_{kh}^{(-l-m)}t_{hi}^{(l)}}{(U+l\omega)(U+n\omega)[U+(n-m)\omega]} \\
& + 2 \sum_{h \neq ijk} \frac{[t_{ij}^{(l)}t_{jk}^{(-l-m)} + t_{ij}^{(-l-m)}t_{jk}^{(l)}]t_{kh}^{(m-n)} + t_{ij}^{(m-n)}t_{jk}^{(l)}t_{kh}^{(-l-m)}}{(U+l\omega)(U-n\omega)(U-m\omega)}t_{hi}^{(n)} \\
& + \sum_{h \neq ijk} \frac{t_{ij}^{(m-n)}t_{jk}^{(-l-m)}t_{kh}^{(l)}t_{hi}^{(n)} + t_{ij}^{(n)}t_{jk}^{(l)}t_{kh}^{(-l-m)}t_{hi}^{(m-n)}}{(U+l\omega)(U-n\omega)(U-m\omega)}. \quad (39)
\end{aligned}$$

The above expression is derived under an assumption $t_{ji}^{(n)} = t_{ij}^{(n)}(-1)^n$, which holds for monochromatic laser lights. In particular, the chiral coupling of crucial interest reads, for the present square lattice with second-neighbour hopping,

$$J_{i,i+y,i+x}^\chi = J_\chi = 2J'_\chi + 2J''_\chi, \quad (40)$$

$$\begin{aligned}
J_{i-x,i,i+x+y}^\chi = & J'_\chi = 4t_0^2t_0'^2 \sum_{lmn} \sin \frac{m\pi}{2} \\
& \times \left[\frac{D_{m-l}}{m\omega} + (D_{m-l} + 2D_{n-l})D_{n-m} \right] D_{n+m} \\
& \times \left[\mathcal{J}_{l+m}(\sqrt{2}A)\mathcal{J}_{l-m}(\sqrt{2}A)\mathcal{J}_{n+m}(A)\mathcal{J}_{n-m}(A) \right. \\
& \left. + \mathcal{J}_{n+m}(\sqrt{2}A)\mathcal{J}_{n-m}(\sqrt{2}A)\mathcal{J}_{l+m}(A)\mathcal{J}_{l-m}(A) \right], \quad (41)
\end{aligned}$$

$$\begin{aligned}
J_{i-x,i-y,i+x}^\chi = & J''_\chi = 4t_0^2t_0'^2 \sum_{lmn} \sin \frac{(3m+2n)\pi}{4} \\
& \times \left[D_l D_n D_{n-m} + (D_l D_{-n} + D_{-n} D_{-n+m})D_{l+m-n} \right] \\
& \times \left[\mathcal{J}_{-l-m}(A)\mathcal{J}_l(A)\mathcal{J}_{m-n}(\sqrt{2}A)\mathcal{J}_n(\sqrt{2}A) \right. \\
& \left. + \mathcal{J}_{m-n}(A)\mathcal{J}_n(A)\mathcal{J}_{-l-m}(\sqrt{2}A)\mathcal{J}_l(\sqrt{2}A) \right], \quad (42)
\end{aligned}$$

where $D_n = (U + n\omega)^{-1}$.

2. Gutzwiller projection

The ground-state property of the system is here analysed using the mean-field approximation with the Gutzwiller ansatz^{29,32}. Namely, we consider an ansatz of the form,

$$|\Psi\rangle = \hat{P}_G |\Psi_0\rangle, \quad (43)$$

$$|\Psi_0\rangle = \prod_{\mathbf{k}} (u_{\mathbf{k}} + v_{\mathbf{k}} \hat{c}_{\mathbf{k}\uparrow}^\dagger \hat{c}_{-\mathbf{k}\downarrow}^\dagger) |0\rangle, \quad (44)$$

with $\hat{P}_G = \prod_i (1 - \hat{n}_{i\uparrow}\hat{n}_{i\downarrow})$ being the Gutzwiller projection. Here, $\hat{c}_{\mathbf{k}\sigma} = N^{-1/2} \sum_i \hat{c}_{i\sigma} e^{-i\mathbf{k}\cdot\mathbf{R}_i}$ with N being the number of lattice sites. The ground state within this ansatz can be obtained by minimising the expectation value,

$$E_0 = \frac{\langle \Psi | \hat{H}_F | \Psi \rangle}{\langle \Psi | \Psi \rangle} = \frac{\langle \hat{P}_G \hat{H}_F \hat{P}_G \rangle_0}{\langle \hat{P}_G \rangle_0}. \quad (45)$$

To evaluate the Gutzwiller projection approximately, we here replace the expectation value with the site-diagonal ones. Namely, we decompose the projection operator as

$$\hat{P}_G = \sum_{c_1, \dots, c_N = h, \uparrow, \downarrow} \left(\prod_{i=1}^N \hat{P}_{ic_i} \right) \quad (46)$$

with $\hat{P}_{ih} \equiv (1 - \hat{n}_{i\uparrow})(1 - \hat{n}_{i\downarrow})$, $\hat{P}_{i\sigma} \equiv n_{i\sigma}(1 - n_{i\bar{\sigma}})$. Then we can evaluate the denominator as

$$\langle \hat{P}_G \rangle_0 \simeq \sum_{c_1, \dots, c_N = h, \uparrow, \downarrow} \prod_{i=1}^N \langle \hat{P}_{ic_i} \rangle_0 \quad (47)$$

$$= \frac{N!}{(N\delta)!(Nf)!(Nf)!} (\bar{f}\bar{f})^{N\delta} (f\bar{f})^{Nf} (f\bar{f})^{Nf} \quad (48)$$

$$\sim \frac{(\bar{f}\bar{f})^{N\delta} (f\bar{f})^{Nf} (f\bar{f})^{Nf}}{\delta^{N\delta} f^{Nf} \bar{f}^{Nf}} = (\bar{f}^2 \delta^{-1})^{N\delta} \bar{f}^{2Nf}, \quad (49)$$

where $f = (1 - \delta)/2$, $\bar{f} = (1 + \delta)/2$, and we have used $n! \sim (n/e)^n$ in the last line. We can evaluate the numerators in the same manner. For the hopping, exchange, and spin-dependent three-site terms, we obtain, respectively,

$$\langle \hat{P}_G \hat{c}_{i\sigma}^\dagger \hat{c}_{j\sigma} \hat{P}_G \rangle_0 \simeq (\bar{f}^2 \delta^{-1})^{N\delta-1} \bar{f}^{2Nf-1} \langle \bar{f} \hat{c}_{i\sigma}^\dagger \hat{c}_{j\sigma} \bar{f} \rangle_0 \quad (50)$$

$$= \frac{2\delta}{1+\delta} \langle \hat{c}_{i\sigma}^\dagger \hat{c}_{j\sigma} \rangle_0 \langle \hat{P}_G \rangle_0, \quad (51)$$

$$\langle \hat{P}_G \hat{S}_i \cdot \hat{S}_j \hat{P}_G \rangle_0 \simeq (\bar{f}^2 \delta^{-1})^{N\delta} \bar{f}^{2Nf-2} \langle \hat{S}_i \cdot \hat{S}_j \rangle_0 \quad (52)$$

$$= \frac{4}{(1+\delta)^2} \langle \hat{S}_i \cdot \hat{S}_j \rangle_0 \langle \hat{P}_G \rangle_0, \quad (53)$$

$$\langle \hat{P}_G \hat{c}_{i\sigma}^\dagger \hat{c}_{j\sigma'} \hat{S}_k \hat{P}_G \rangle_0 \simeq (\bar{f}^2 \delta^{-1})^{N\delta-1} \bar{f}^{2Nf-2} \langle \bar{f} \hat{c}_{i\sigma}^\dagger \hat{c}_{j\sigma'} \bar{f} \hat{S}_k \rangle_0 \quad (54)$$

$$= \frac{4\delta}{(1+\delta)^2} \langle \hat{c}_{i\sigma}^\dagger \hat{c}_{j\sigma'} \hat{S}_k \rangle_0 \langle \hat{P}_G \rangle_0. \quad (55)$$

We also obtain $\langle \hat{P}_G \hat{S}_i \cdot (\hat{S}_j \times \hat{S}_k) \hat{P}_G \rangle_0 \simeq [8/(1+\delta)^3] \langle \hat{S}_i \cdot (\hat{S}_j \times \hat{S}_k) \rangle_0 \langle \hat{P}_G \rangle_0$ in the same manner.

The remaining terms have an ambiguity in determining the Gutzwiller factor, because they are accompanied by the density operator $\hat{P}_G \hat{n}_i \hat{P}_G = \hat{P}_G [\sum_\sigma \hat{n}_{i\sigma} (1 - \hat{n}_{i\bar{\sigma}})] \hat{P}_G$, which can be regarded either as an operator or a constant $\langle \hat{n}_{i\sigma} (1 - \hat{n}_{i\bar{\sigma}}) \rangle_0 \simeq f\bar{f}$, in the above scheme. Here, we discard the second-order fluctuation around the expectation value, $(\hat{n}_{i\sigma} - f)(1 - \hat{n}_{i\bar{\sigma}} - \bar{f})$, to approximate the projected density operator as $\sum_\sigma \hat{n}_{i\sigma} (1 - \hat{n}_{i\bar{\sigma}}) \simeq \hat{n}_i \delta + 2f^2$. Then the Gutzwiller factors for the remaining terms are evaluated as

$$\begin{aligned}
\langle \hat{P}_G \hat{n}_i \hat{n}_j \hat{P}_G \rangle_0 & \simeq \frac{4}{(1+\delta)^2} \langle (\hat{n}_i \delta + 2f^2)(\hat{n}_j \delta + 2f^2) \rangle_0 \langle \hat{P}_G \rangle_0 \\
& = \frac{4\delta^2}{(1+\delta)^2} \langle \hat{n}_i \hat{n}_j \rangle_0 \langle \hat{P}_G \rangle_0 + \frac{2\delta(1-\delta)^2}{(1+\delta)^2} \langle \hat{n}_i + \hat{n}_j \rangle_0 \langle \hat{P}_G \rangle_0 + \text{const.}, \quad (56)
\end{aligned}$$

$$\begin{aligned}
\langle \hat{P}_G \hat{c}_{i\sigma}^\dagger \hat{c}_{j\sigma} \hat{n}_k \hat{P}_G \rangle_0 &\simeq \frac{4\delta}{(1+\delta)^2} \langle \hat{c}_{i\sigma}^\dagger \hat{c}_{j\sigma} (\hat{n}_k \delta + 2f^2) \rangle_0 \langle \hat{P}_G \rangle_0 \\
&= \frac{4\delta^2}{(1+\delta)^2} \langle \hat{c}_{i\sigma}^\dagger \hat{c}_{j\sigma} \hat{n}_k \rangle_0 \langle \hat{P}_G \rangle_0 + \frac{2\delta(1-\delta)^2}{(1+\delta)^2} \langle \hat{c}_{i\sigma}^\dagger \hat{c}_{j\sigma} \rangle_0 \langle \hat{P}_G \rangle_0.
\end{aligned} \tag{57}$$

Note that the density-density term is known to have small effects in the variational Monte Carlo calculation in the low-doping regime, with which the present treatment is consistent.

With these expressions, the minimisation of E_0 turns out to be reduced to that of $\langle \hat{H}_{F0} \rangle_0$, where \hat{H}_{F0} is the Hamiltonian with the modified coupling constant but without the Gutzwiller projection, as given by

$$\begin{aligned}
\hat{H}_{F0} &= -g\delta \sum_{ij\sigma} \left[\tilde{t}_{ij} + \frac{(1-\delta)^2}{2(1+\delta)} \sum_k \Gamma_{ijk} \right] \hat{c}_{i\sigma}^\dagger \hat{c}_{j\sigma} \\
&+ \frac{g^2}{2} \sum_{ij} J_{ij} \left(\hat{\mathbf{S}}_i \cdot \hat{\mathbf{S}}_j - \frac{\delta^2}{4} \hat{n}_i \hat{n}_j \right) + \frac{g^3}{6} \sum_{ijk} J_{ijk}^\chi (\hat{\mathbf{S}}_i \times \hat{\mathbf{S}}_j) \cdot \hat{\mathbf{S}}_k \\
&+ g^2\delta \sum_{ijk\sigma\sigma'} \Gamma_{ijk} \left[(\hat{c}_{i\sigma}^\dagger \sigma_{\sigma\sigma'} \hat{c}_{j\sigma'}) \cdot \hat{\mathbf{S}}_k - \frac{\delta}{2} \delta_{\sigma\sigma'} \hat{c}_{i\sigma}^\dagger \hat{c}_{j\sigma} \hat{n}_k \right]
\end{aligned} \tag{58}$$

with $g = 2/(1+\delta)$. Differentiating $\langle \hat{H}_{F0} \rangle_0$ by $u_{\mathbf{k}}, v_{\mathbf{k}}$ in Eq. (44), we arrive at the Bogoliubov-de Gennes Hamiltonian Eq. (8) in the main text. In particular, the detailed form for the present system is given as

$$\begin{aligned}
\varepsilon(\mathbf{k}) &= -\mu + \frac{1}{2} \varepsilon_x (\cos k_x + \cos k_y) + \varepsilon_{x+y} \cos k_x \cos k_y \\
&- 4g\delta(1-\delta) \text{Re} \Gamma_{i-x-y, i+x, i} (\cos 2k_x \cos k_y + \cos k_x \cos 2k_y) \\
&- g\delta(1-\delta) \text{Re} (2\Gamma_{i-x, i+x, i+y} + \Gamma_{i-x, i+x, i}) (\cos 2k_x + \cos 2k_y) \\
&- 2g\delta(1-\delta) \text{Re} \Gamma_{i-x-y, i+x+y, i} \cos 2k_x \cos 2k_y \\
&+ \frac{3}{2} g^3 J'_\chi \text{Re} (\Delta^* \Delta') (\cos 2k_x \cos k_y + \cos k_x \cos 2k_y), \tag{59}
\end{aligned}$$

$$\begin{aligned}
\varepsilon_x &= -4g\delta\tilde{t} - \frac{3-\delta^2}{2} g^2 J\chi_x - 8g\delta(1-\delta) \text{Re} \Gamma_{i-x, i, i+y} \\
&- 2g^2\delta(3-\delta) \text{Re} (2\Gamma_{i-x, i+y, i} + \Gamma_{i-x, i+x, i}) \chi_x \\
&- 4g^2\delta(3-\delta) \text{Re} (\Gamma_{i-x, i, i+y} + \Gamma_{i-x-y, i+x, i}) \chi_{x+y} \\
&+ \frac{3}{2} g^3 \text{Re} [2J'_\chi \Delta'^* + J'_\chi \Delta' (\Delta_{x+2y}^* - \Delta_{2x+y}^*)], \tag{60}
\end{aligned}$$

$$\begin{aligned}
\varepsilon_{x+y} &= -4g\delta\tilde{t}' - \frac{3-\delta^2}{2} g^2 J'\chi_{x+y} - 4g\delta(1-\delta) \text{Re} \Gamma_{i-x, i+y, i} \\
&- 2g^2\delta(3-\delta) \text{Re} (2\Gamma_{i-x, i+x, i+y} + \Gamma_{i-x-y, i+x+y, i}) \chi_{x+y} \\
&- 4g^2\delta(3-\delta) \text{Re} (\Gamma_{i-x, i, i+y} + \Gamma_{i-x-y, i+x, i}) \chi_x \\
&- \frac{3}{2} g^3 \text{Re} [2J''_\chi \Delta_{2x}^* \Delta' - iJ'_\chi \Delta^* (\Delta_{2x+y} + \Delta_{x+2y})], \tag{61}
\end{aligned}$$

$$\begin{aligned}
F(\mathbf{k}) &= \frac{1}{2} F_x (\cos k_x - \cos k_y) + i F_{x+y} \sin k_x \sin k_y \\
&+ \frac{3g^3 J''_\chi}{2} \Delta' \chi_{x+y} (\cos 2k_x - \cos 2k_y) \\
&- \frac{3ig^3 J'_\chi}{2} \Delta \chi_{x+y} (\sin 2k_x \sin k_y + \sin k_x \sin 2k_y) \\
&- \frac{3g^3 J'_\chi}{2} \chi_x \Delta' (\cos k_x \cos 2k_y - \cos 2k_x \cos k_y), \tag{62}
\end{aligned}$$

$$\begin{aligned}
F_x &= g^2 \left[\frac{3+\delta^2}{2} J - 2\delta(3+\delta) \text{Re} (2\Gamma_{i-x, i+y, i} - \Gamma_{i-x, i+x, i}) \right] \Delta \\
&- g^2 \left[4\delta(3+\delta) \gamma + 3gJ_\chi \chi_x + \frac{3}{2} gJ'_\chi (\chi_{2x+y} + \chi_{x+2y}) \right] \Delta' \\
&- \frac{3}{2} ig^3 J'_\chi (\Delta_{2x+y} + \Delta_{x+2y}) \chi_{x+y}, \tag{63}
\end{aligned}$$

$$\begin{aligned}
F_{x+y} &= g^2 \left[4\delta(3+\delta) \gamma + 3gJ_\chi \chi_x + \frac{3}{2} gJ'_\chi (\chi_{2x+y} + \chi_{x+2y}) \right] \Delta \\
&- g^2 \left[\frac{3+\delta^2}{2} J' - 2\delta(3+\delta) \text{Re} (2\Gamma_{i-x, i+x, i+y} - \Gamma_{i-x-y, i+x+y, i}) \right] \Delta' \\
&- \frac{3}{2} g^3 [J'_\chi \chi_x (\Delta_{2x+y} - \Delta_{x+2y}) + 2J''_\chi \Delta_{2x} \chi_{x+y}]. \tag{64}
\end{aligned}$$

When Δ is real, we can further simplify the expressions using $\chi_{mx+ny} = \chi_{nx+my}$ and $\Delta_{mx+ny}^* = -\Delta_{nx+my}^*$, after which the first line of F_{x+y} gives $\delta F^{xy}(\mathbf{k})$ in the main text.

ACKNOWLEDGMENTS

S.K. acknowledges JSPS KAKENHI Grant 20K14407, and CREST (Core Research for Evolutional Science and Technology; Grant number JPMJCR19T3) for support. H.A. thanks CREST (Grant Number JPMJCR18T4), and JSPS KAKENHI Grant JP17H06138.

¹ I. Prigogine, “From being to becoming: time and complexity in the physical sciences,” (Freeman, 1980).

² T. Oka and H. Aoki, “Photovoltaic Hall effect in graphene,” *Phys.*

Rev. B **79**, 081406 (2009), Erratum: **79**, 169901(E) (2009).

³ T. Oka and H. Aoki, “Photovoltaic Berry curvature in the honeycomb lattice,” *Journal of Physics: Conference Series* **200**, 062017

- (2010).
- ⁴ T. Oka and H. Aoki, “All optical measurement proposed for the photovoltaic Hall effect,” *Journal of Physics: Conference Series* **334**, 012060 (2011).
 - ⁵ F. D. M. Haldane, “Model for a quantum Hall effect without Landau levels: Condensed-matter realization of the “parity anomaly,”” *Phys. Rev. Lett.* **61**, 2015 (1988).
 - ⁶ T. Kitagawa, T. Oka, A. Brataas, L. Fu, and E. Demler, “Transport properties of nonequilibrium systems under the application of light: Photoinduced quantum Hall insulators without Landau levels,” *Phys. Rev. B* **84**, 235108 (2011).
 - ⁷ J. W. McIver, B. Schulte, F.-U. Stein, T. Matsuyama, G. Jotzu, G. Meier, and A. Cavalleri, “Light-induced anomalous Hall effect in graphene,” *Nat. Phys.* **16**, 38 (2019).
 - ⁸ T. Mikami, S. Kitamura, K. Yasuda, N. Tsuji, T. Oka, and H. Aoki, “Brillouin-Wigner theory for high-frequency expansion in periodically driven systems: Application to Floquet topological insulators,” *Phys. Rev. B* **93**, 144307 (2016), Erratum: **99**, 019902(E) (2019).
 - ⁹ S. Takayoshi, H. Aoki, and T. Oka, “Magnetization and phase transition induced by circularly polarized laser in quantum magnets,” *Phys. Rev. B* **90**, 085150 (2014).
 - ¹⁰ S. Takayoshi, M. Sato, and T. Oka, “Laser-induced magnetization curve,” *Phys. Rev. B* **90**, 214413 (2014).
 - ¹¹ S. Kitamura, T. Oka, and H. Aoki, “Probing and controlling spin chirality in Mott insulators by circularly polarized laser,” *Phys. Rev. B* **96**, 014406 (2017).
 - ¹² M. Claassen, H.-C. Jiang, B. Moritz, and T. P. Devereaux, “Dynamical time-reversal symmetry breaking and photo-induced chiral spin liquids in frustrated Mott insulators,” *Nat. Commun.* **8** (2017), 10.1038/s41467-017-00876-y.
 - ¹³ N. Tsuji, T. Oka, P. Werner, and H. Aoki, “Dynamical band flipping in fermionic lattice systems: An ac-field-driven change of the interaction from repulsive to attractive,” *Phys. Rev. Lett.* **106**, 236401 (2011).
 - ¹⁴ S. Kitamura and H. Aoki, “ η -pairing superfluid in periodically-driven fermionic Hubbard model with strong attraction,” *Phys. Rev. B* **94**, 174503 (2016).
 - ¹⁵ S.-L. Zhang, L.-J. Lang, and Q. Zhou, “Chiral d -wave superfluid in periodically driven lattices,” *Phys. Rev. Lett.* **115**, 225301 (2015).
 - ¹⁶ K. Takasan, A. Daido, N. Kawakami, and Y. Yanase, “Laser-induced topological superconductivity in cuprate thin films,” *Phys. Rev. B* **95**, 134508 (2017).
 - ¹⁷ H. Chono, K. Takasan, and Y. Yanase, “Laser-induced topological s -wave superconductivity in bilayer transition metal dichalcogenides,” *Phys. Rev. B* **102**, 174508 (2020).
 - ¹⁸ U. Kumar and S.-Z. Lin, “Inducing and controlling superconductivity in the Hubbard honeycomb model using an electromagnetic drive,” *Phys. Rev. B* **103**, 064508 (2021).
 - ¹⁹ H. Dehghani, M. Hafezi, and P. Ghaemi, “Light-induced topological superconductivity via Floquet interaction engineering,” *Phys. Rev. Research* **3**, 023039 (2021).
 - ²⁰ T. Oka and S. Kitamura, “Floquet engineering of quantum materials,” *Annu. Rev. Condens. Matter Phys.* **10**, 387 (2019).
 - ²¹ L. D’Alessio and M. Rigol, “Long-time behavior of isolated periodically driven interacting lattice systems,” *Phys. Rev. X* **4**, 041048 (2014).
 - ²² A. Lazarides, A. Das, and R. Moessner, “Equilibrium states of generic quantum systems subject to periodic driving,” *Phys. Rev. E* **90**, 012110 (2014).
 - ²³ M. Bukov, L. D’Alessio, and A. Polkovnikov, “Universal high-frequency behavior of periodically driven systems: from dynamical stabilization to Floquet engineering,” *Adv. Phys.* **64**, 139 (2015).
 - ²⁴ A. Eckardt and E. Anisimovas, “High-frequency approximation for periodically driven quantum systems from a Floquet-space perspective,” *New J. Phys.* **17**, 093039 (2015).
 - ²⁵ T. Mori, T. Kuwahara, and K. Saito, “Rigorous bound on energy absorption and generic relaxation in periodically driven quantum systems,” *Phys. Rev. Lett.* **116**, 120401 (2016).
 - ²⁶ T. Kuwahara, T. Mori, and K. Saito, “Floquet–Magnus theory and generic transient dynamics in periodically driven many-body quantum systems,” *Ann. Phys. (N.Y.)* **367**, 96 (2016).
 - ²⁷ J. H. Mentink, K. Balzer, and M. Eckstein, “Ultrafast and reversible control of the exchange interaction in Mott insulators,” *Nat. Commun.* **6**, 6708 (2015).
 - ²⁸ M. Bukov, M. Kolodrubetz, and A. Polkovnikov, “Schrieffer-Wolff transformation for periodically driven systems: Strongly correlated systems with artificial gauge fields,” *Phys. Rev. Lett.* **116**, 125301 (2016).
 - ²⁹ M. Ogata and H. Fukuyama, “The t - J model for the oxide high- T_c superconductors,” *Rep. Prog. Phys.* **71**, 036501 (2008).
 - ³⁰ D. H. Dunlap and V. M. Kenkre, “Dynamic localization of a charged particle moving under the influence of an electric field,” *Phys. Rev. B* **34**, 3625 (1986).
 - ³¹ A. Eckardt, M. Holthaus, H. Lignier, A. Zenesini, D. Ciampini, O. Morsch, and E. Arimondo, “Exploring dynamic localization with a Bose-Einstein condensate,” *Phys. Rev. A* **79**, 013611 (2009).
 - ³² M. Ogata and A. Himeda, “Superconductivity and antiferromagnetism in an extended Gutzwiller approximation for t - J model: Effect of double-occupancy exclusion,” *J. Phys. Soc. Jpn.* **72**, 374 (2003).
 - ³³ F. Peronaci, M. Schiró, and M. Capone, “Transient dynamics of d -wave superconductors after a sudden excitation,” *Phys. Rev. Lett.* **115**, 257001 (2015).
 - ³⁴ R. Matsunaga, N. Tsuji, H. Fujita, A. Sugioka, K. Makise, Y. Uzawa, H. Terai, Z. Wang, H. Aoki, and R. Shimano, “Light-induced collective pseudospin precession resonating with Higgs mode in a superconductor,” *Science* **345**, 1145 (2014).
 - ³⁵ R. Shimano and N. Tsuji, “Higgs mode in superconductors,” *Annu. Rev. Condens. Matter Phys.* **11**, 103 (2020).
 - ³⁶ K. Katsumi, N. Tsuji, Y. I. Hamada, R. Matsunaga, J. Schneeloch, R. D. Zhong, G. D. Gu, H. Aoki, Y. Gallais, and R. Shimano, “Higgs mode in the d -wave superconductor $\text{Bi}_2\text{Sr}_2\text{CaCu}_2\text{O}_{8+x}$ driven by an intense Terahertz pulse,” *Phys. Rev. Lett.* **120**, 117001 (2018).
 - ³⁷ L. Schwarz, B. Fauseweh, N. Tsuji, N. Cheng, N. Bittner, H. Krull, M. Berciu, G. S. Uhrig, A. P. Schnyder, S. Kaiser, and D. Manske, “Classification and characterization of nonequilibrium Higgs modes in unconventional superconductors,” *Nat. Commun.* **11** (2020), 10.1038/s41467-019-13763-5.
 - ³⁸ M. Budden, T. Gebert, M. Buzzi, G. Jotzu, E. Wang, T. Matsuyama, G. Meier, Y. Laplace, D. Pontiroli, M. Riccò, F. Schlawin, D. Jaksch, and A. Cavalleri, “Evidence for metastable photo-induced superconductivity in K_3C_{60} ,” *Nat. Phys.* **17**, 611 (2021), and refs. therein.
 - ³⁹ M. Knap, M. Babadi, G. Refael, I. Martin, and E. Demler, “Dynamical Cooper pairing in nonequilibrium electron-phonon systems,” *Phys. Rev. B* **94**, 214504 (2016).
 - ⁴⁰ M. Babadi, M. Knap, I. Martin, G. Refael, and E. Demler, “Theory of parametrically amplified electron-phonon superconductivity,” *Phys. Rev. B* **96**, 014512 (2017).
 - ⁴¹ Y. Murakami, N. Tsuji, M. Eckstein, and P. Werner, “Nonequilibrium steady states and transient dynamics of conventional superconductors under phonon driving,” *Phys. Rev. B* **96**, 045125 (2017).

- ⁴² D. M. Kennes, M. Claassen, M. A. Sentef, and C. Karrasch, “Light-induced d -wave superconductivity through Floquet-engineered Fermi surfaces in cuprates,” [Phys. Rev. B **100**, 075115 \(2019\)](#).
- ⁴³ Y.-F. Jiang and H.-C. Jiang, “Topological superconductivity in the doped chiral spin liquid on the triangular lattice,” [Phys. Rev. Lett. **125**, 157002 \(2020\)](#).